

THE INTERSTELLAR MEDIUM OF IRAS 08572+3915 NW: H_3^+ AND WARM HIGH-VELOCITY CO^{1,2}

T. R. GEBALLE,³ M. GOTO,⁴ T. USUDA,⁵ T. OKA,⁶ AND B. J. McCALL⁷

Received 2005 December 7; accepted 2006 February 28

ABSTRACT

We confirm the first detection of the molecular ion H_3^+ in an extragalactic object, the highly obscured ultraluminous galaxy IRAS 08572+3915 NW. We also have detected absorption lines of the fundamental band of CO in this galaxy. The CO absorption consists of a cold component close to the systemic velocity and warm, highly blueshifted and redshifted components. The warm blueshifted component is remarkably strong and broad and extends at least to -350 km s^{-1} . Some analogies can be drawn between the H_3^+ and cold CO in IRAS 08572+3915 NW and the same species seen toward the Galactic center. The profiles of the warm CO components are not those expected from a dusty torus of the type thought to obscure active galactic nuclei. They are probably formed close to the dust continuum surface near the buried and active nucleus and are probably associated with an unusual and energetic event there.

Subject headings: galaxies: active — galaxies: individual (IRAS 08572+3915) — galaxies: ISM — infrared: galaxies — line: profiles — molecular processes

1. INTRODUCTION

Ultraluminous infrared galaxies (ULIRGs) have been extensively studied at all wavelengths from the radio to X-ray in order to probe the nature of the energy source—starburst and/or active galactic nucleus (AGN). Numerous investigators have concluded that ULIRGs are mainly found in interacting systems (e.g., Sanders & Mirabel 1996; Veilleux et al. 2002 and references therein). However, in the many cases where the nuclear regions are heavily obscured it is still unclear whether their huge luminosities are the result of greatly enhanced nuclear star formation, greatly enhanced accretion by a central black hole, or both. Infrared spectroscopy potentially has an important role to play in this investigation, as it can probe regions close to the nucleus at high angular resolution and detect diagnostics unique to each phenomenon, as well as discern the nature of the interstellar medium of the ULIRG more distant from the nucleus. Recent observations using this technique include the measurements of broad-line regions and coronal lines, which are signposts of AGNs, in several ULIRGs (Veilleux et al. 1999; Murphy et al. 2001), the detection of interstellar aromatic hydrocarbon features and hydrogen recombination lines indicative of massive star formation (Imanishi & Dudley 2000; Soifer et al. 2002; Dannerbauer et al. 2005) in a partially intersecting set of ULIRGs, and most recently and perhaps most remarkably, the discovery of CO in dense and warm gas close to the central luminosity source of the $z = 0.327$ ULIRG, IRAS F00183–7111 (Spoon et al. 2004).

H_3^+ , the highly reactive molecular ion on which interstellar gas phase chemistry is based (Herbst & Klemperer 1973; Watson 1973), is a potentially useful infrared spectroscopic tool for study-

ing the interstellar gas in distant galaxies. It is important observationally for understanding both dark and diffuse interstellar clouds (Geballe 2000). In both types of clouds it is produced following cosmic-ray ionization of H_2 to H_2^+ , which quickly reacts with H_2 to form H_3^+ . The steady state abundance of H_3^+ is very low, because it is destroyed readily in dark clouds by reactions with neutral molecules (principally CO) and atoms (mainly O) and even more readily in diffuse clouds by dissociative recombination with electrons, which, due to the photoionization of carbon, are much more abundant than in dark clouds. The absorption strengths of H_3^+ lines provide basic information on the cloud dimensions and environment, in addition to temperature. The observed column density of H_3^+ can directly yield the product of the distance through the cloud and the cosmic-ray ionization rate in the cloud. This is because, unlike most other molecules, the number density of H_3^+ in a cloud is a constant that depends only on the ionization rate of H_2 and whether the cloud is dark or diffuse. This unusual property of H_3^+ comes about because its creation rate per unit volume is proportional to the first power of the cloud density, rather than to the square.

The detection of strong H_3^+ absorption toward the center of the Galaxy (Geballe et al. 1999) suggests that it also should be possible to detect H_3^+ in the interstellar medium of suitable external galaxies—those with sufficiently bright and compact sources of infrared continuum radiation and large column densities of interstellar molecular gas along their lines of sight. One of the most promising galaxies for an H_3^+ search is the ULIRG IRAS 08572+3915. Images at several wavelengths of this interacting pair of galaxies can be found in Evans et al. (2002). The $3.4 \mu\text{m}$ interstellar hydrocarbon absorption observed by Wright et al. (1996) and Imanishi & Dudley (2000; see also Fig. 1, this paper) in the northwest component of this merging galaxy pair is deeper than that observed toward the Galactic center. In the Galaxy this feature signifies extinction by dust in diffuse clouds. The $10 \mu\text{m}$ silicate absorption toward IRAS 08572+3915 NW (Dudley & Wynn-Williams 1997; Spoon et al. 2006a) also is among the strongest detected, although no absorption due to water ice is present at $3.1 \mu\text{m}$ (Imanishi et al. 2006). In addition, IRAS 08572+3915 NW possesses intense CO line emission at millimeter wavelengths (Sanders et al. 1989; Evans et al. 2002). Thus, extensive columns of diffuse and dense gas exist in front of the nuclear infrared source of IRAS 08572+3915 NW, which may contain a buried AGN (Dudley & Wynn-Williams 1997; Imanishi &

¹ Based on data obtained at the United Kingdom Infrared Telescope, which is operated by the Joint Astronomy Center on behalf of the UK Particle Physics and Astronomy Research Council.

² Based on data collected at the Subaru Telescope, which is operated by the National Astronomical Observatory of Japan.

³ Gemini Observatory, 670 North A'ohoku Place, Hilo, HI 96720; tgeballe@gemini.edu.

⁴ Max Planck Institute for Astronomy, Koenigstuhl 17, D-69117, Heidelberg, Germany.

⁵ Subaru Telescope, Astronomical National Observatory of Japan, 650 North A'ohoku Place, Hilo, HI 96720.

⁶ Department of Astronomy and Astrophysics, Department of Chemistry, 5735 South Ellis Avenue; and Enrico Fermi Institute, University of Chicago, Chicago, IL 60637.

⁷ Department of Chemistry and Department of Astronomy, University of Illinois, Urbana, IL 61801.

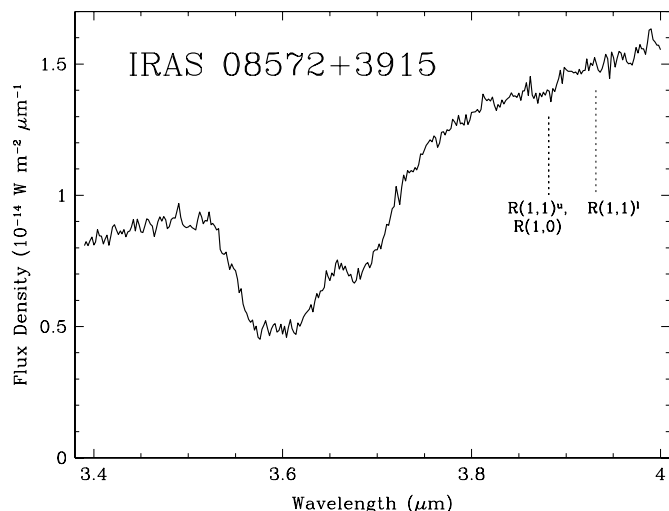


FIG. 1.—The 3.4–4.0 μm spectrum of IRAS 08572+3915 NW at $R \sim 1500$ showing the redshifted 3.4 μm interstellar hydrocarbon band and the locations of the lines of H_3^+ detected at higher resolution. The noise can be estimated by the fluctuations in $\sim 0.05 \mu\text{m}$ wide intervals.

Dudley 2000), although this interpretation has been contested (Arribas et al. 2000).

Here we report confirmation of the detection of H_3^+ in IRAS 08572+3915 NW reported by Geballe (2001). To gain additional information about the interstellar medium of this galaxy, we also obtained a spectrum of it in the region of the fundamental band of carbon monoxide. This spectrum reveals both a cold interstellar component, possibly associated with some of the gas containing the detected H_3^+ , and an unusual warm and dense component superficially similar to that observed toward IRAS F00183–7111 by Spoon et al. (2004). Here, however, the CO band is resolved into individual lines, and the lines themselves are velocity resolved, revealing remarkably broad and high-speed components.

A data log of the observations reported below is provided in Table 1. In all cases data reduction was straightforward, involving removal of bad frames, extraction of spectra from co-added two-dimensional spectral images, wavelength calibration using arc lamps and telluric absorption lines, despiking, division by a telluric standard star observed at close to the same air mass and reduced in a similar fashion, and flux calibration using the observed or predicted flux density of the standard.

2. OBSERVATIONS AND RESULTS

2.1. H_3^+

An initial search for H_3^+ in IRAS 08572+3915 NW was made in 1998 December at the United Kingdom Infrared Telescope

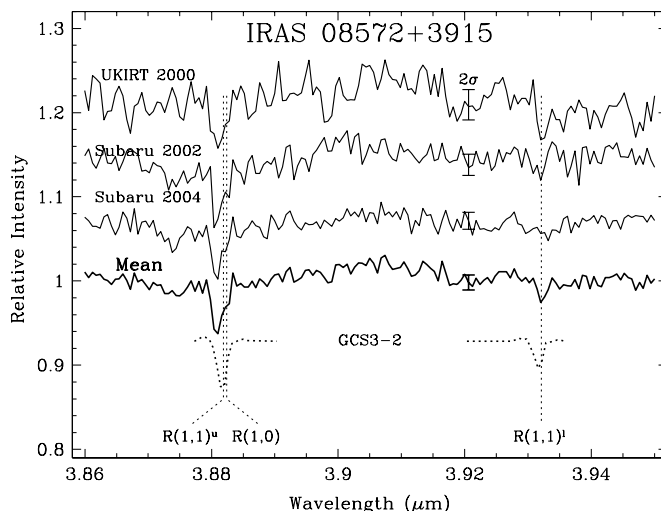


FIG. 2.—Individual and mean spectra from UKIRT and Subaru of IRAS 08572+3915 NW near the locations of three lines of H_3^+ . The high-resolution spectrum of the $R(1, 1)^r$ line in the Galactic center source GCS3-2 (Oka et al. 2005), binned to the same point-to-point spacing as the spectra of IRAS 08572+3915 NW, is shown at lower right and also was used to make a model spectrum of the 3.88 μm doublet at lower left.

(UKIRT) with the use of the facility spectrograph CGS4 (Mountain et al. 1990), employed at a resolving power of 1500 and covering 3.4–4.0 μm . No H_3^+ lines were detected. This spectrum is shown in Figure 1, because it is a better quality spectrum of the redshifted 3.4 μm hydrocarbon absorption feature in IRAS 08572+3915 NW than those published to date (Imanishi & Dudley 2000; Mason et al. 2004; Imanishi et al. 2006). The spectrum also illustrates the difficulty of detecting weak lines from the ground at medium spectral resolution in the thermal infrared region.

In 2000 December a 3.82–3.98 μm spectrum of IRAS 08572+3915 NW was obtained at UKIRT, with CGS4 configured to give a higher resolving power of 6000. The spectrum covered the wavelength range of three lines of H_3^+ from the lowest lying ortho and para levels. These are the $R(1, 1)^o$ – $R(1, 0)$ doublet at 3.66808 and 3.66852 μm (separated by 36 km s^{-1}), whose mean wavelength is redshifted to 3.8822 μm , and the $R(1, 1)^r$ singlet at 3.71548 μm , redshifted to 3.9321 μm . We use $z = 0.0583$, which was determined from the CO pure rotational 1–0 line (Evans et al. 2002) and is probably accurate to better than 0.0001 (30 km s^{-1}), as the nominal systemic redshift and express all wavelengths in vacuo. The relevant portion of the spectrum is shown at the top of Figure 2. Statistically significant absorption features were observed at the expected wavelengths of the lines, indicating that the molecular ion had been detected (Geballe 2001). The H_3^+ search was repeated in 2002 and 2004 at the Subaru

TABLE 1
OBSERVING LOG

UT Date	Telescope	Wavelength (μm)	R	Exposure (minutes)	Weather	Calibrating Star
19981227.....	UKIRT	3.39–4.00	1500	78	Clear	HR 3690 (A3 V)
20001208.....	UKIRT	3.82–3.99	6000	130	Clear	HR 2818 (A1 V)
20010109.....	UKIRT	4.89–5.06	7500	90	Clear	HR 3579 (F5 V)
20020224.....	Subaru	3.85–3.96	10000	67	Clear	HD 90470 (A2 V) ^a
20040209.....	Subaru	3.85–3.96	5000	80	Clouds	HR 2891 (A1 V)
20040402.....	Subaru	3.85–3.96	10000	92	Clear	HR 2891 (A1 V)

^a Calibration star observed on different date due to rapid change in weather.

TABLE 2
 H_3^+ LINE EQUIVALENT WIDTHS

Feature	Wavelength (μm)	W_λ
$R(1, 1)^u + R(1, 0)$	3.88139	$(1.44 \pm 0.14) \times 10^{-4}$
$R(1, 1)^l$	3.9322	$(0.39 \pm 0.12) \times 10^{-4}$

Telescope using its Infrared Camera and Spectrograph (IRCS; Tokunaga et al. 1998; Kobayashi et al. 2000) at resolving powers of 10,000 and 5000. These data, each summed in $0.0006 \mu\text{m}$ ($\sim 50 \text{ km s}^{-1}$) wide bins to match the UKIRT point spacing, also are shown in Figure 2 and, except for the singlet in the 2004 spectrum, also contain modest signal-to-noise ratio detections of these lines. In the 2004 data the signal near the wavelength of the singlet is depressed as expected, but it is also depressed at adjacent wavelengths.

The transmission spectrum of the earth's atmosphere in the $3.86\text{--}3.95 \mu\text{m}$ interval contains about 50 narrow and roughly evenly spaced absorption lines from high-altitude N_2O . In unratiod spectra with the above binning the strongest of these are 20% deep. Any effects due to noncancellation of these lines would result in systematic features of comparable strengths at many wavelengths in the ratioed spectra. No evidence for any such features is present in any of the individual spectra. The broad and very shallow emission bump centered near $3.908 \mu\text{m}$ in each spectrum in Figure 2 is due to absorption by $\text{H I } 15\text{--}6$ in the spectra of the A dwarf telluric standards.

The mean of the three spectra is shown near the bottom of Figure 2. In it the detection of the doublet is convincing, whereas that of the singlet is marginal (at about 3σ). Relative to the systemic velocity, the centroids of the doublet and the singlet correspond to LSR velocities of $-50 \pm 30 \text{ km s}^{-1}$ and $+10 \pm 50 \text{ km s}^{-1}$, respectively. Thus, there is some disagreement in the velocities of the two features, but it is within the uncertainties, which are due to possible errors in the wavelength calibration, the uncertain relative contributions of the components of the doublet, and the noise in the spectrum. The uncertainty in the wavelength scale is determined largely by the UKIRT spectrum and conservatively is 10 km s^{-1} . The uncertainty in the centroid of the doublet depends on the width and signal-to-noise ratio of the feature and on the relative contributions of the two lines (separated by 36 km s^{-1} , which is roughly 1 : 1 in Galactic dark clouds; McCall et al. 1999) toward the Galactic center (Oka et al. 2005). The uncertainty due to the feature's profile and signal-to-noise ratio is about 20 km s^{-1} , whereas reasonable variation in the ratio of the doublet's components translates into an uncertainty of about 5 km s^{-1} in the centroid. Thus, the overall uncertainty in the velocity centroid of the doublet is about 30 km s^{-1} . For the marginally detected singlet the uncertainty in the centroid due to the noise is at least equal to the point spacing, which is 46 km s^{-1} (this can be seen by comparing the centroids of the UKIRT 2000 and Subaru 2002 spectra), giving an overall uncertainty in the velocity centroid of roughly 50 km s^{-1} for that line.

Although the moderate discrepancy in velocities suggests the possibility that the weak absorption at $3.932 \mu\text{m}$ is a noise fluctuation and that the much stronger $3.882 \mu\text{m}$ absorption feature has an identification other than H_3^+ , we believe that this is unlikely. First, we have found no other viable candidate for the $3.882 \mu\text{m}$ absorption other than H_3^+ . Second, in the numerous Galactic sources in which this doublet has been detected there is no evidence of contamination of the doublet by other lines. Third, we expect to detect H_3^+ at roughly this strength toward

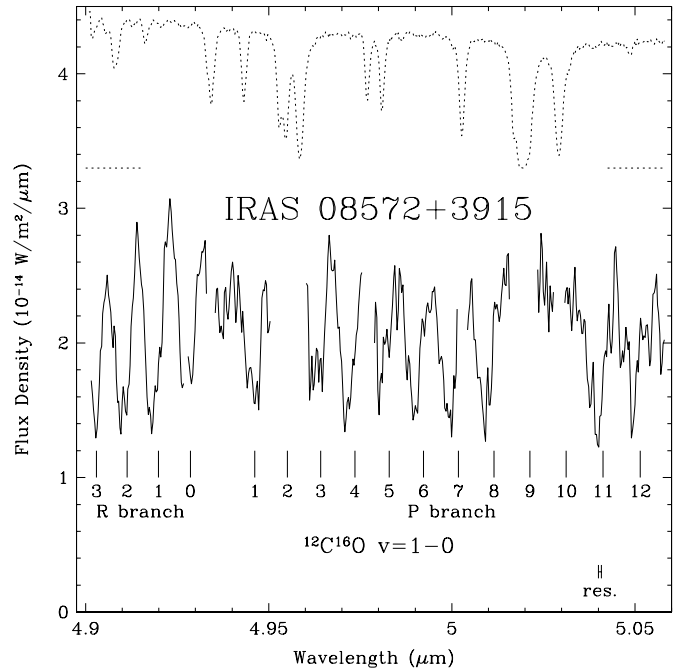


FIG. 3.—Spectrum of IRAS 08572+3915 NW at $R = 7500$ covering a portion of the fundamental band of CO. The atmospheric transmission is shown as a dashed line. CO $v = 1\text{--}0$ band line positions are indicated at the bottom, for a redshift of 0.05821.

IRAS 08572+3915, based on the heavy obscuration of the nuclear source and the evidence for a high column density of diffuse interstellar gas and by analogy with the Galactic center. Finally, the radial velocity of the $3.88 \mu\text{m}$ absorption, if due to H_3^+ , is the same (to within the uncertainties) as that of the peak absorption by cold CO discussed in the next subsection.

The equivalent widths of the two features are given in Table 2. Their uncertainties are based on average point-to-point fluctuations in the spectrum near the lines. The $3.88 \mu\text{m}$ doublet has more than 3 times the equivalent width of the singlet. Using the standard equations relating column density to equivalent width (Geballe & Oka 1996), we derive column densities of $(1.8 \pm 0.6) \times 10^{15} \text{ cm}^{-2}$ in the (1, 1) para level and $(2.6 \pm 0.6) \times 10^{15} \text{ cm}^{-2}$ in the (1, 0) ortho level. The most likely values yield a formal excitation temperature of 100 K, but this result is highly uncertain, mainly due to the large uncertainty in the equivalent width of the singlet. At densities typical of molecular clouds the total H_3^+ column density is the sum of the above values, $4.4 \times 10^{15} \text{ cm}^{-2}$. If the temperature is significantly higher than 100 K and the clouds are diffuse, a few higher levels can be significantly populated and the total column density of H_3^+ could be higher, as shown by Oka & Epp (2004). In the Galactic Center, where much of the H_3^+ is in clouds at temperatures of $\sim 250 \text{ K}$, the total column density of $4.3 \times 10^{15} \text{ cm}^{-2}$ is 1/4 greater than the sum of the column densities in these lowest ortho and para levels (Oka et al. 2005).

2.2. CO

Figure 3 shows the $4.90\text{--}5.05 \mu\text{m}$ spectrum of IRAS 08572+3915 NW observed at a resolving power of 7500. The spectrum is noisy, and several intervals within it are unrecoverable due to strong telluric absorption lines. However, it is clear that the spectrum contains strong and broad absorption lines of the fundamental band of CO, stretching across the entire observed interval. Indeed, the lines are so broad that in some portions of the

spectrum it is unclear whether continuum gaps exist between them. The spacing of lines of the 1–0 band of CO is typically 550 km s^{-1} . The apparent elevation of the continuum near $4.92 \mu\text{m}$ might be due to $\text{H I Pa}\beta$, which is redshifted to $4.925 \mu\text{m}$, although the line appears to be considerably wider than that of shorter wavelength infrared H I recombination lines observed by Goldader et al. (1995) and Veilleux et al. (1999).

The centroids of the CO lines in IRAS 08572+3915 NW are considerably blueshifted from the central wavelengths determined from the systemic redshift of the galaxy. Moreover, although the signal-to-noise ratio of the spectrum is low, careful examination of Figure 3 suggests that the lines from the lower rotational levels are broader than those from high J . To better test whether a separate velocity component is present in the low J lines, we have co-added the spectra of the $R(1)$, $R(2)$, and $P(1)$ lines, as well as those of the $P(6)$, $P(8)$, and $P(11)$ lines, the lines least affected by telluric absorption. These average, low J , and high J spectra are compared in Figure 4. The low J line profiles have two strong absorption maxima, at approximately -50 ± 25 and $-150 \pm 25 \text{ km s}^{-1}$ relative to the systemic velocity, whereas only a single strong absorption maximum, at $-160 \pm 25 \text{ km s}^{-1}$, is present for the high J profiles. Thus, roughly speaking there is a warm blueshifted CO absorption component extending roughly from 0 to -350 km s^{-1} and a cold component centered near 0 km s^{-1} , at approximately the same radial velocity as the H_3^+ lines. A warm redshifted component, which appears to be present in the mean high J profile in Figure 4, has recently been confirmed by M. Shirahata et al. (2006, in preparation). In the UKIRT spectrum it is centered at $+100 \pm 30 \text{ km s}^{-1}$ and is considerably weaker and narrower than the other two components.

There is little or no evidence for CO absorption or emission from vibrationally excited states. The $v = 2-1$ $R(6)$ transition ($4.939 \mu\text{m}$), which occurs at the CO $v = 1-0$ band center, corresponds to a marginal depression in the continuum between the strong CO 1–0 lines. However, the continuum levels between the 1–0 lines at 5.02 and $5.06 \mu\text{m}$, where the $v = 2-1$ line wavelengths lie midway between the 1 and 0 lines, are comparable to the levels between the 1–0 lines at $4.96-4.99 \mu\text{m}$, where the 2–1 line wavelengths coincide with the 1–0 lines.

The characteristic CO temperatures and column densities are difficult to determine accurately from the narrow spectral range observed. Strong blueshifted absorption lines are present at all observed J levels (up to 12), implying that the warm blueshifted CO component is close to or in LTE and that either the blueshifted portions of the medium J lines are optically thick or the blueshifted gas has a range of temperatures. It appears that the line from the highest J level observed, the $P(12)$ line, is somewhat weaker than the lines from lower levels. This and the estimated strength of the $R(0)$ and $P(1)$ blue components allow us to crudely and tentatively estimate the mean temperature of the warm blueshifted component to be $200 (+100, -50) \text{ K}$. Insufficient information is available to estimate the temperature of the weak redshifted component, but it may be warmer than the blueshifted component.

Assuming an isothermal optically thin slab in this temperature range, the column density of the warm blueshifted component is $2 \times 10^{18} \text{ cm}^{-2}$, with an uncertainty of a factor of 2. However, it is almost certainly an oversimplification to regard the warm absorbing gas as isothermal and optically thin at all velocities. As discussed in § 3.2, the profile is probably made up of spatially separated velocity components. If each of these is absorbing along a different line of sight to a different location on the continuum source, the actual line optical depths are considerably

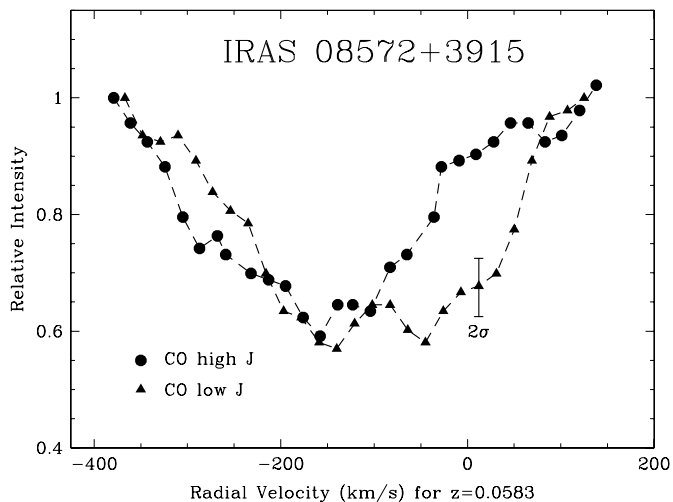


FIG. 4.—Velocity profiles of CO lines from low and high J levels. Circles are the mean of the 1–0 $R(1)$, $R(2)$, and $P(1)$ lines; triangles indicate the mean of the $P(6)$, $P(8)$, and $P(11)$ lines. A representative error bar ($\pm 1 \sigma$) is shown.

greater than in the above estimate. A column density an order of magnitude higher than the above value would not be surprising.

This argument may also apply to the column density of the cold low-velocity absorption component. Based on its strength and small number of rotational levels that are populated, the column density of this component is probably several times less than that of the warm blueshifted component. The column density of the warm redshifted component is even less. Assuming $[\text{CO}]/[\text{H}_2] = 1.5 \times 10^{-4}$ (Lee et al. 1996), the lower limit on the hydrogen column density associated with the observed CO (assuming the lines are optically thin) is $N(\text{H}_2) \approx 1.5 \times 10^{22} \text{ cm}^{-2}$. By comparison, from the peak optical depth of 4.2 in the $10 \mu\text{m}$ silicate absorption feature (Spoon et al. 2006a) and using $A_V/\tau_{\text{sil}} = 17.5$ (Roche & Aitken 1984; Rieke & Lebofsky 1985) and $N_{\text{H}} = 1.9 \times 10^{21} \text{ cm}^{-2} \text{ mag}^{-1}$, we obtain $N(\text{H}_2) = 7 \times 10^{22} \text{ cm}^{-2}$, which is also a lower limit because of the possibility of radiative transfer effects and/or foreground silicate emission.

3. DISCUSSION

3.1. Low-Velocity H_3^+ and CO

The velocity of the H_3^+ is close to the systemic velocity of IRAS 08572+3915 NW, as indicated in Figure 2. Although the absorption lines of H_3^+ appear fairly simple in shape, the low signal-to-noise ratio and low resolution could be masking many details. Figure 2 includes the spectrum toward the Galactic center source GCS3-2 recently observed at 6 km s^{-1} resolution by Oka et al. (2005), but shown here with the same binning as the IRAS 08572+3915 NW spectra. Oka et al. (2005) found that the spectrally resolved profile of GCS3-2 has a full width at zero intensity (FWZI) of 150 km s^{-1} and at least six discrete velocity components, from both diffuse and dark clouds, some within a few tens of parsecs of the center and some in distant spiral arms. The H_3^+ absorption line profiles toward IRAS 08572+3915 NW could be similarly complex.

The presence of a strong $3.4 \mu\text{m}$ interstellar feature suggests that a considerable fraction of the interstellar molecular gas along the line of sight toward the nuclear continuum source of IRAS 08572+3915 NW is in diffuse clouds, as is the case toward the Galactic center (Whittet et al. 1997). If so and assuming that the total column density of H_3^+ is not greatly different from the

sum of the column densities in the lowest ortho and para levels, $4.4 \times 10^{15} \text{ cm}^2$, we can estimate the column length of absorbing H₃⁺ from its steady state density in diffuse clouds. The value of $n(\text{H}_3^+)$ depends on the assumed cosmic-ray ionization rate, ζ . Assuming the previously canonical value of $\sim 1 \times 10^{-7} \text{ cm}^{-3}$ for $n(\text{H}_3^+)$ in diffuse clouds (McCall et al. 1998; Geballe et al. 1999) obtained if $\zeta = 3 \times 10^{-17} \text{ s}^{-1}$, the derived length of the column containing H₃⁺ in IRAS 08572+3915 NW is ~ 10 kpc, which clearly is unrealistically long. A similar unreasonably high result is obtained for the Galactic center (Geballe et al. 1999). Using the 40 times higher cosmic-ray ionization rate found in one galactic diffuse cloud, but suspected of existing in many or all such clouds (McCall et al. 2003), reduces the path length to a still high, but more reasonable, 300 pc. In the Galactic center Oka et al. (2005) have found that the ionization rate is even several times higher than this value. If conditions in IRAS 08572+3915 NW are similar, the path length then would be reduced to less than 100 pc. If, instead, all of the H₃⁺ were found in dense clouds, the path length through them would be ~ 10 pc, but it then would be difficult to explain the absence of H₃⁺ in the diffuse clouds that produce the strong $3.4 \mu\text{m}$ feature. Moreover, the extinction through the dense cloud material to the continuum source would be unrealistically high, ~ 1000 mag, based on the rough Galactic ratio $N(\text{H}_3^+)/A_V$ of $3.6 \times 10^{12} \text{ cm}^{-2} \text{ mag}^{-1}$ reported by Oka et al. (2005). Thus, we conclude that the bulk of the observed H₃⁺ is located in diffuse molecular gas.

The absorption lines of H₃⁺ and the cold CO have similar velocity ranges. However, as in the case of the Galactic center (Oka et al. 2005), they probably do not arise in all of the same clouds. The CO abundance in diffuse clouds is only 1% of the carbon abundance, whereas in dense clouds almost all carbon is in CO. Thus, the absorption by cold CO must occur primarily in dense clouds, whereas, as argued above, the lines of H₃⁺ are probably formed mainly in diffuse clouds. The present CO data do not allow much to be inferred about the dense clouds, although they do suggest from the width of the cold component that, as in the case of the Galactic center, there are several of them along the line of sight.

3.2. High-Velocity CO

The discovery of high-velocity CO features is the most striking result of this paper. Clearly, there is no physical relation whatsoever between the dominant blueshifted CO absorption and the H₃⁺. This is because (1) highly blueshifted velocities are not seen in the H₃⁺ lines, despite the large CO column density in that component, and (2) the column density of blueshifted H₃⁺ must be very low, because the length of the column of blueshifted CO is very short, as discussed below.

The existence in the high-velocity gas of strong CO lines from levels as high as $J = 12$ implies that the CO rotational population is maintained in LTE to at least that level. Using our crude determination of 200 K for the kinetic temperature and equating the Einstein A coefficient for the $J = 12-11$ transition (eq. [1] in Thompson 1973) to the collisional excitation rate, assuming a cross section for collisional excitation by H₂ of $1 \times 10^{-15} \text{ cm}^2$ (e.g., McKee et al. 1982), we estimate that the gas density $n(\text{H}_2)$ must be at least $3 \times 10^6 \text{ cm}^{-3}$. For $[\text{CO}]/[\text{H}_2] = 1.5 \times 10^{-4}$ (Lee et al. 1996), the lower limit to the observed warm CO column density of $2 \times 10^{18} \text{ cm}^{-2}$ implies that the overall column length of warm CO is less than 0.001 pc, or less than 0.01 pc for an order of magnitude higher CO column density. The H₃⁺ column density expected in such short column lengths would be undetectable.

Confinement of the observed wide range of blueshifted velocities to a single clump of gas that is this thin and is detached

from the continuum source is inconsistent with the observations. Collisions between portions of the gas in the clump at relative velocities of more than 10 km s^{-1} would heat the gas significantly above the observed temperatures, and collisions at more than several tens of km s^{-1} would dissociate even the CO. Yet there is no evidence in our spectra for the CO being vibrationally excited. Thus, if the absorbing gas is detached, it must be composed of numerous well-separated thin sheets of dense gas, each of which contains a narrow range of velocities.

It is simpler to account for the wide range of blueshifted velocities if the line-forming CO is located on the outer surface of an expanding, more or less spherical, optically thick continuum source. In such a geometry a range of absorption velocities would be present, from near zero near the edges of the source to most highly blueshifted at the center. This simple model implies an expansion velocity of $\sim 350 \text{ km s}^{-1}$ and a column density much higher than the lower limit given in § 2.2.

This model cannot account for the weak redshifted CO absorption component seen at $+100 \text{ km s}^{-1}$, however. Judging from the relative strengths of the low and high J absorptions at this velocity (see Fig. 4), the redshifted CO appears warmer than the blueshifted CO and therefore probably is located interior to it. Thus, the actual geometry of the continuum source and the absorbing gas may be quite complex.

3.3. Star Formation or AGN?

It has been argued by Evans et al. (2002) that star formation is rampant in the central regions of IRAS 08572+3915 NW, and thus we consider whether the observed high velocities of the CO lines could be the result of such activity. The mid-infrared continuum of IRAS 08572+3915 NW arises in a region less than 250 pc in diameter (Soifer et al. 2002), and thus the putative young stars would be confined to that region, which is roughly the size of the CO millimeter line emission (Evans et al. 2002). In star-forming regions winds from young stellar objects (YSOs) shock-heat and sweep up cloud material. Veilleux et al. (1999) have detected emission lines in IRAS 08572+3915 NW from the first excited vibrational state of H₂, which could be emitted by shock-heated gas as a result of star formation. The observed absorption by high-velocity CO could arise in numerous dense and thin shells of swept-up postshock gas in a large number of discrete star-forming clouds seen against the continua from a widely distributed set of YSOs. A large preponderance of blueshifted absorption over redshifted absorption would be expected, as is observed.

Despite the above considerations, this explanation of the observed continuum and high-velocity absorption lines as the result of myriads of individual star-forming events over a very extended region seems contrived. Moreover, the mean velocity of the warm blueshifted CO is considerably higher than would be expected based on observations of outflows from YSOs in the Galaxy. A further difficulty with it is that, even in the most active star-forming regions in the Galaxy, such as OMC-1, the bulk of the molecular gas is at temperatures much less than 200 K. Only a small portion of the gas, located just downstream from the shocks, is so warm. However, in IRAS 08572+3915 NW the bulk of the gas producing the absorption lines is at this warm temperature.

Thus, we suspect that events associated with star formation are unlikely to be responsible for the CO line profiles. Adaptive optics imaging on a large telescope of the infrared K -band continuum might provide important information on its spatial distribution and a way of discriminating between domination of the energetics by an extended starburst or a more compact source of radiation.

Imanishi et al. (2001) have claimed that a buried AGN must be the dominant luminosity source of IRAS 08572+3915 NW (and some other ULIRGs). In that case one would expect the infrared continuum source to be compact. The preponderance of blueshifted warm gas in front of the nucleus of IRAS 08572+3915 NW naturally suggests ejection of material from the AGN. The luminosity of the central source is $2 \times 10^{12} L_{\odot}$ (Dudley & Wynn-Williams 1997); hence, the ~ 200 K CO must be ~ 10 pc from the AGN. This size and the observed expansion speed imply that the ejection began $\sim 30,000$ yr ago. If the cloud forms a complete shell around the AGN, the mass of the ejected material exceeds $2000 M_{\odot}$, and the kinetic energy exceeds 3×10^{50} ergs, roughly comparable to the total energy liberated in a supernova.

In the unified model of AGN, the differences between type 1 and type 2 objects is explained by invoking a rotating toroidal cloud of dust and gas that obscures gas in the broad-line region from some viewing angles while leaving it exposed from others. The presence of both blueshifted and redshifted CO absorptions in IRAS 08572+3915 NW suggests the possibility of rotation of the absorbing gas about the central luminosity source. As in the case of expansion, the absorbing CO would need to be situated on the outside surface of the dust in order for red and blueshifted components to be seen in absorption against it. The major problem with this model is the extreme weakness of the redshifted absorption relative to the blueshifted absorption. It implies a highly asymmetric distribution of rotating material, a highly asymmetric distribution of continuum emission, or variation of the foreground extinction by several tens of visual magnitudes across the source of the infrared continuum. The possibility that the redshifted gas is at a higher temperature than the blueshifted gas is a second potential difficulty.

Thus, one cannot easily interpret our observations as arising in a torus-like gaseous structure. We tentatively interpret them as probing a transient event (occurring much more rapidly than the galaxy-galaxy interaction) in the nucleus of IRAS 08572+3915 NW. Neither the consequences of a starburst or “steady state” phenomenon related to an obscured AGN (e.g., a stable torus) can provide an explanation for the CO observations. Although the transient event appears to be mainly one of ejection of material from the nucleus, the simultaneous observation of a small amount of material approaching the nucleus suggests both a complex geometry and complex gas motions.

4. CONCLUSION

The broad absorption lines of CO toward IRAS 08572+3915 NW constitute the most remarkable finding of this paper. The highly velocity-shifted and warm CO implies a transient event in the nucleus, more likely to be associated with AGN activity than with massive star formation. No observations of IRAS 08572+

3915 NW directly related to this phenomenon appear in previously published papers. Warm CO is not unique to this ULIRG, however. Spoon et al. (2004) have found broad absorption due to the fundamental band of CO in IRAS F10183–7111 and have recently reported several similar detections in other deeply obscured galactic nuclei (Spoon et al. 2006b). All of their observations were made at much lower spectral resolution and hence do not resolve individual lines and determine velocities. Thus, it is unclear whether the apparently energetic events taking place in IRAS 08572+3915 NW are also occurring in the other galaxies. In some cases, e.g., IRAS F10183–7111, the CO that Spoon et al. have found is considerably warmer and has a larger column density than IRAS 08572+3915 NW, but their general conclusions about the shortness of the absorbing column and proximity to the central luminosity source are similar to ours.

The absorption lines of H_3^+ toward IRAS 08572+3915 probably arise largely in diffuse gas, as do those seen toward the Galactic center. In combination with the low-velocity low J lines of CO, the H_3^+ could in principle provide much more detailed information on the nature of the interstellar medium of IRAS 08572+3915 NW. However, considerably higher resolution and higher sensitivity measurements than those reported here are required. Sensitive measurements of the $R(2, 2)^l$ and metastable $R(3, 3)^l$ line could much more tightly constrain the density and temperature of the H_3^+ -containing clouds, as they have done for the H_3^+ seen along the line of sight to the Galactic center (Oka et al. 2005).

The detection of extragalactic H_3^+ and the high-resolution infrared spectra of extragalactic CO reported here and by Spoon et al. (2003), which have resolved the fundamental band into individual lines, are the first measurements of their types. In the future, using ground-based 8–10 m class and larger telescopes, along with the *James Webb Space Telescope*, one can anticipate that infrared spectroscopy of interstellar CO and H_3^+ , in combination with measurements of other molecules and dust, will be a standard technique for probing the diffuse and dense clouds and gauging the nuclear activity of many distant galaxies.

We thank the staffs of UKIRT and Subaru for their support. We are grateful to F. Lahuis, M. Shirahata, H. Spoon, and the referee for a number of helpful comments. T. R. G.’s research is supported by the Gemini Observatory, which is operated by the Association of Universities for Research in Astronomy, Inc., on behalf of the international Gemini partnership of Argentina, Australia, Brazil, Canada, Chile, the United Kingdom, and the United States of America. M. G. is supported by a Fellowship for Research Abroad from the Japan Society for the Promotion of Science. T. O. is supported by NSF grant PHY 03-54200.

REFERENCES

- Arribas, S., Colina, L., & Borne, K. D. 2000, *ApJ*, 545, 228
 Dannerbauer, H., Rigopolou, D., Lutz, D., Genzel, R., Sturm, E., & Moorwood, A. F. M. 2005, *A&A*, 441, 999
 Dudley, C. C., & Wynn-Williams, C. G. 1997, *ApJ*, 488, 720
 Evans, A. S., Mazzarella, J. M., Surace, J. A., & Sanders, D. B. 2002, *ApJ*, 580, 749
 Geballe, T. R. 2000, *Philos. Trans. R. Soc. London, A*, 358, 2503
 ———. 2001, in *IAP Colloq. 17, Gaseous Matter in Galaxies and Intergalactic Space*, ed. R. Ferlet, J.-M. Desert, & B. Raban (Paris: Frontier Group), 231
 Geballe, T. R., McCall, B. J., Hinkle, K. H., & Oka, T. 1999, *ApJ*, 510, 251
 Geballe, T. R., & Oka, T. 1996, *Nature*, 384, 334
 Goldader, J. D., Joseph, R. D., Doyon, R., & Sanders, D. B. 1995, *ApJ*, 444, 97
 Herbst, E., & Klemperer, W. 1973, *ApJ*, 185, 505
 Imanishi, M., & Dudley, C. C. 2000, *ApJ*, 545, 701
 Imanishi, M., Dudley, C. C., & Maloney, P. R. 2001, *ApJ*, 558, L93
 Imanishi, M., Dudley, C. C., & Maloney, P. R. 2006, *AJ*, 637, 114
 Kobayashi, N., et al. 2000, *Proc. SPIE*, 4008, 1056
 Lee, H.-H., Bettens, R. P. A., & Herbst, E. 1996, *A&AS*, 119, 111
 Mason, R. E., Wright, G., Pendleton, Y., & Adamson, A. 2004, *ApJ*, 613, 770
 McCall, B. J., Geballe, T. R., Hinkle, K. H., & Oka, T. 1998, *Science*, 279, 1910
 ———. 1999, *ApJ*, 522, 338
 McCall, B. J., et al. 2003, *Nature*, 422, 500
 McKee, C. F., Storey, J. W. V., Watson, D. M., & Green, S. 1982, *ApJ*, 259, 647
 Mountain, C. M., Robertson, D., Lee, T. J., & Wade, R. 1990, *Proc. SPIE*, 1235, 25
 Murphy, T. W., Soifer, B. T., Matthews, K., Armus, L., & Kiger, J. R. 2001, *AJ*, 121, 97
 Oka, T., & Epp, E. 2004, *ApJ*, 613, 349
 Oka, T., Geballe, T. R., Goto, M., Usuda, T., & McCall, B. J. 2005, *ApJ*, 632, 882
 Rieke, G. H., & Lebofsky, M. J. 1985, *ApJ*, 288, 618

- Roche, P. F., & Aitken, D. K. 1984, *MNRAS*, 208, 481
- Sanders, D. B., & Mirabel, I. F. 1996, *ARA&A*, 34, 749
- Sanders, D. B., Scoville, N. Z., Zensus, A., Soifer, B. T., Wilson, T. L., Zylka, R., & Steppe, H. 1989, *A&A*, 213, L5
- Soifer, B. T., Neugebauer, G., Matthews, K., Egami, E., & Weinberger, A. J. 2002, *AJ*, 124, 2980
- Spoon, H. W. W., Moorwood, A. F. M., Pontoppidan, K. M., Cami, J., Kregel, M. Lutz, D., & Tielens, A. G. G. M. 2003, *A&A*, 402, 499
- Spoon, H. W. W., et al. 2004, *ApJS*, 154, 184
- . 2006a, *ApJ*, 2006, *ApJ*, 638, 759
- . 2006b, in *IAU Symp. 231, Astrochemistry throughout the Universe: Recent Successes and Current Challenges*, ed. D. C. Lis, G. A. Blake, & E. Herbst (Cambridge: Cambridge Univ. Press), in press
- Thompson, R. I. 1973, *ApJ*, 181, 1039
- Tokunaga, A. T., et al. 1998, *Proc. SPIE*, 3354, 512
- Veilleux, S., Kim, D.-C., & Sanders, D. B. 2002, *ApJS*, 143, 315
- Veilleux, S., Sanders, D. B., & Kim, D.-C. 1999, *ApJ*, 522, 139
- Watson, W. D. 1973, *ApJ*, 183, L17
- Whittet, D. C. B., et al. 1997, *ApJ*, 490, 729
- Wright, G. S., Bridger, A., Geballe, T. R., & Pendleton, Y. 1996, in *New Extragalactic Perspectives in the New South Africa*, ed. D. L. Block & J. M. Greenberg (Dordrecht: Kluwer), 143